

# Fluidization of Mixtures of Two Solids: A Unified Model of the Transition to the Fluidized State

B. Formisani, R. Girimonte, and V. Vivacqua

Departmento di Ingegneria Chimica e dei Materiali, Università della Calabria, I 87030 Arcavacata di Rende (Cosenza), Italy

DOI 10.1002/aic.13876

Published online July 10, 2012 in Wiley Online Library (wileyonlinelibrary.com).

*Fluidization of binary beds of dissimilar solids has place along a fluidization velocity interval bounded by the “initial” and the “final fluidization velocity” of the mixture, with segregation phenomena that continuously change the internal distribution of its components. Varying with the relative importance of size and density differences between components, the fluidization process may follow more than one mechanism, depending on whether the process of fluidization starts from bed top or bottom. It is shown how, irrespective of the fluidization pattern exhibited by the two-solid system, the limiting velocities of its fluidization interval can be calculated with good accuracy by the same relationships, derived from the analysis of the fluidization force equilibrium. The model proposed provides a unique theoretical frame for the analysis of the fluidization behavior of any two-solid system and encompasses as a particular case the behavior of simpler mixtures, whose components differ only in density or size. © 2012 American Institute of Chemical Engineers AIChE J, 59: 729–735, 2013*

**Keywords:** fluidization, solid mixtures, segregation, mixing, modeling

## Introduction

In a recent article,<sup>1</sup> a model derived from fundamental analysis has been developed, capable to interpret the fluidization properties of homogeneous beds of two solids subjected to either density or size segregation of their components. A key feature of the approach followed, widely supported by previous work in the field,<sup>2–5</sup> is that of characterizing the behavior of binary particle systems by the two limiting velocities of the fluidization process, namely the “initial” and the “final fluidization velocity” of the mixture, hereafter referred to as  $u_{if}$  and  $u_{ff}$ , respectively.

Although not thoroughly predictive as regards the calculation of  $u_{ff}$ , the relationships proposed accurately reproduce the dependence of either characteristic velocity on solid properties and mixture composition. This seems a promising result in view of further investigations aimed at establishing a quantitative relationship between the regime of fluidization and the state of mixing or segregation of bed components. To pursue this objective, however, the validity of the theory proposed has to be checked on a wider variety of systems. Reproducing the behavior of binary beds whose solids differ only in density or size proves useful to enlighten the action of either segregation factor by a separate analysis; systems of this kind, however, seldom represent, on their own, cases of practical interest. More frequently, two-component beds used in process industry are made of solids of different nature and size that form mixtures of various compositions.

With beds of fully dissimilar solids, both the density and the size difference are at work in promoting component separation. Their simultaneous action may give place to a reinforced tendency of the fluidized bed to form segregated layers or to a relative balance of the two driving forces of segregation. As a consequence, different fluidization patterns are observed, which are made of a succession of mixing-segregation equilibria determined by the relative weight assumed by either factor, as discussed in previous works of our research group.<sup>1,2</sup> Such a multiplicity of behavior greatly complicates the problem of setting up models or relationships of general validity to describe the dynamics of segregating fluidization. Attempts made so far to achieve this objective by empirical approaches have been unsuccessful, given that an important aspect of the problem is that of grasping the common features of the different phenomenologies of fluidization. As this article intends to show, however, fundamental analysis provides the tools to encompass the whole spectrum of fluidization behaviors exhibited by homogeneous beds of two solids in a unique theoretical frame.

## Alternative Fluidization Patterns: Top and Bottom Fluidization

Mixtures of two solids that differ both in density and size undergo, when gradually fluidized from  $u_{if}$  to  $u_{ff}$ , a succession of mixing-segregation equilibria determined by the simultaneous action of both segregation factors. When differences of density and size act synergistically with respect to the phenomenon, that is, when the less dense component is also the smaller, the mechanism of fluidization is that sketched in Figure 1, hereafter indicated as “top fluidization.” Like in the case of simple density- or size-segregating

Correspondence concerning this article should be addressed to B. Formisani at [bruno.formisani@unical.it](mailto:bruno.formisani@unical.it).

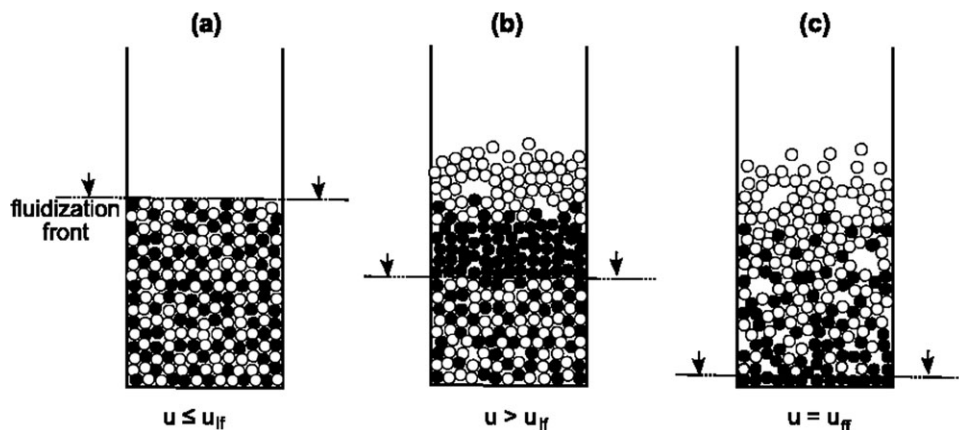


Figure 1. Binary fluidization pattern: top fluidization.

systems, a fluidization front is generated at the upper surface of the bed at  $u_{if}$  (Figure 1a) and travels downward as much as the gas velocity is increased. Lighter and smaller particles (the “flotsam” component, after the definition of Rowe et al.<sup>6</sup>) gather up on top of the bed and form a bubbling layer, while jetsam ones form a fixed stratum underneath. Over  $u_{if}$ , the height of the original homogeneous mixture lying at the bottom of the column, not yet fluidized, progressively decreases (Figure 1b). Once that  $u$  equals mixture  $u_{ff}$ , the whole bed mass is suspended and the final pressure drop level is attained, while the two solids achieve a degree of mixing higher than that observed at lower velocities (Figure 1c), variable with the specific mixture and with its composition. In all cases, however, a top layer of practically pure flotsam is observed.

Conversely, with binary systems whose denser component is also the smaller, more than one fluidization pattern is possible. If the denser solid achieves fluidization first (a case that occurs whenever its size is sufficiently smaller than that of the other), the fluidization front develops at the bottom of the bed and the whole phenomenology is somewhat reversed, so that it can be referred to as “bottom fluidization.” As soon as the gas velocity reaches  $u_{if}$  of the mixture, the whole bed is first raised bodily so that a tiny horizontal gap is created between it and the gas distributor. The particles with the lower minimum fluidization velocity (the “fluidized” component) rain down and start forming a bubbling layer at the base of the column (see Figure 2b); at the same time, the other component gathers up as a fixed layer on top of the original mixture, which rests between the two segregated strata. Further increases of  $u$  promote the growth of the two segregated

layers at the expenses of the mixed portion of the bed until, at  $u_{ff}$  and over, the whole bed is supported by the gas and the two solids mix up again up to a certain limit (Figure 2c).

Thus, as long as  $u$  varies in the interval bounded by  $u_{if}$  and  $u_{ff}$ , three distinct layers are distinguishable, according to the schematization of Figure 3 (see Ref. 1 for a detailed description): the fluidized layer, the residual mixed bed, and the packed layer, whose heights are  $h_f$ ,  $h_m$ , and  $h_p$ , respectively. The mechanism of fluidization changes the order in which they follow one after another from top to bottom, with the upper layer constituted by the fluidized solid or by the packed one.

## Model Equations

Although fluidization of a bed of monodisperse solids can be modeled as a stepwise event occurring at the incipient fluidization velocity of the system, a binary mixtures achieves the fully suspended state through an extended transient that requires crossing a discrete velocity interval. Defining the boundaries of this interval, that is, the “initial” and the “final fluidization velocity” of the mixture, has therefore the same meaning than calculating the minimum fluidization velocity of a monocomponent system.<sup>2-4</sup>

During the process of binary fluidization, one of the two solids, hereafter called the “fluidized” component,<sup>6</sup> achieves the suspended state first, whereas the other, the “packed” one, requires a higher velocity level to leave the fixed state. With simple mixtures (i.e., when the two solids differ either in density or size) as well as with some beds of dissimilar solids, the terms “fluidized” and “packed” are equivalent to the more popular “flotsam” and “jetsam,” in common use to indicate the material that gathers up, respectively, at the top

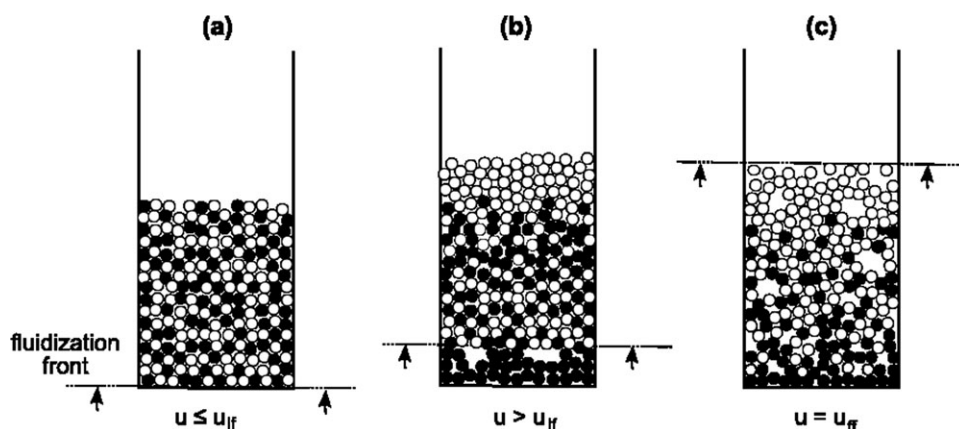
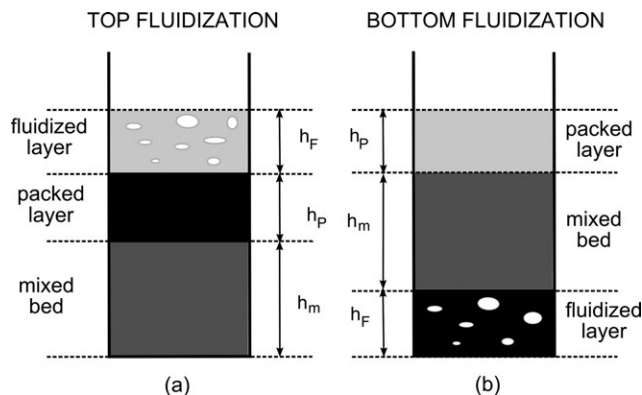


Figure 2. Binary fluidization pattern: bottom fluidization.



**Figure 3. Three layers structures of mixtures of thoroughly dissimilar solids.**

or the bottom of the bed. Of the two terminologies, the former appears preferable as it covers also the case, encountered in the present investigation, in which the component that forms the top layer, and hence the flotsam, is fluidized last.

### The initial fluidization velocity

Of the two velocities  $u_{if}$  and  $u_{ff}$ , the former is more easily calculated, as definition of the equilibrium between gaseous drag and buoyant weight only requires the knowledge of the properties of the fixed bed, whose mixing state is known. As demonstrated in a previous work,<sup>2</sup>  $u_{if}$  of a bed of two solid species initially well mixed is obtained from the equation of the force balance on the three sections of the bed

$$\frac{180\mu_g u_{if} (1 - \varepsilon_{mf})^2}{d_{av}^2 \varepsilon_{mf}^3} = (\rho_{av} - \rho_g)(1 - \varepsilon_{mf})g \quad (1)$$

where  $d_{av}$  and  $\rho_{av}$  are the average Sauter diameter and the average particle density, respectively, defined as

$$\frac{1}{d_{av}} = \frac{x_F}{d_F} + \frac{1 - x_F}{d_P} \quad (2)$$

$$\rho_{av} = \rho_F x_F + \rho_P (1 - x_F) \quad (3)$$

In these relationships,  $x_F$  is the volumetric fraction of the fluidized component in the packed bed. Its value, therefore, represents the composition of the whole mixture at velocities lower than  $u_{if}$  as well as that of the portion of it not yet fluidized at velocities higher than  $u_{if}$  but lower than  $u_{ff}$ .

Once that the value of bed voidage  $\varepsilon_{mf}$ , drawn from the experimental curve of  $\varepsilon_{mf,m}$  vs.  $x_F$ , is substituted into Eq. 1 together with Eqs 2 and 3, the relationship can be used as a fully predictive tool for calculating  $u_{if}$ .

### The final fluidization velocity

As regards the calculation of  $u_{ff}$ , the procedure used to set up the force balance, analogous to that followed in the aforementioned article,<sup>1</sup> does not require knowing in advance whether the mixture will undergo top or bottom fluidization as it equally applies to each of the two structures sketched in Figure 3. During the fluidization transient from  $u_{if}$  to  $u_{ff}$ , the total drag force on the three layers of the binary bed is calculated, irrespective of their mutual position, as

$$F_D = \frac{180\mu_g u (1 - \varepsilon_{mf,P})^2}{d_P^2 \varepsilon_{mf,P}^3} A h_P + \frac{180\mu_g u (1 - \varepsilon_{mf,m})^2}{d_{av}^2 \varepsilon_{mf,m}^3} A h_m + \frac{180\mu_g u (1 - \varepsilon_{mf,F})^2}{d_F^2 \varepsilon_{mf,F}^3} A h_F \quad (4)$$

while the buoyant weight is

$$W = \{(\rho_P - \rho_g)(1 - \varepsilon_{mf,P})h_P + (1 - \varepsilon_{mf,m})h_m[(\rho_F - \rho_g)x_F + (\rho_P - \rho_g)(1 - x_F)] + (\rho_F - \rho_g)(1 - \varepsilon_{mf,F})h_F\}Ag \quad (5)$$

By assuming that the hold up of bubbles in the fluidized layer does not significantly change its height, so that

$$\frac{180\mu_g u (1 - \varepsilon_{mf,F})^2}{d_F^2 \varepsilon_{mf,F}^3} A h_F = (\rho_F - \rho_g)(1 - \varepsilon_{mf,F})h_F Ag \quad (6)$$

and considering that the growth of the packed layer over  $u_{if}$  is related to the parallel reduction of the height of the residual portion of the original mixture by the mass balance

$$(1 - \varepsilon_{mf,P})h_P = (1 - \varepsilon_{mf,m})(h_0 - h_m)(1 - x_F) \quad (7)$$

equating the relationships Eqs. 4 and 5 with the substitution of Eqs. 6 and 7 yields the following expression:

$$u_{ff} = \frac{[(\rho_F - \rho_g)x_F h_m + (\rho_P - \rho_g)(1 - x_F)h_0]g}{180\mu_g \left[ \frac{(1 - \varepsilon_{mf,m})}{(\varepsilon_{mf,m}^3 d_{av}^2)} h_m + \frac{(1 - \varepsilon_{mf,P})}{(\varepsilon_{mf,P}^3 d_P^2)} (h_0 - h_m)(1 - x_F) \right]} \quad (8)$$

which renders the final fluidization velocity of the mixture in function of the constitutive properties of its two components, as well as of the overall volumetric fraction of the fluidized component.  $u_{ff}$  is thus related to the extent of segregation, measured by the height  $h_m$  of the residual portion of the original mixture at the moment the bed is fully supported by the upwelling gas.

Given that the minimum fluidization velocity of each of the two solids is calculated as

$$u_{mf,F/P} = \frac{(\rho_{F/P} - \rho_g)d_{F/P}^2 \varepsilon_{mf,F/P}^3 g}{180\mu_g (1 - \varepsilon_{mf,F/P})} \quad (9)$$

substitution of Eq. 9 into Eq. 8 provides as an alternative expression of the final fluidization velocity

$$u_{ff} = \frac{u_{mf,F} \frac{(1 - \varepsilon_{mf,F})}{(\varepsilon_{mf,F}^3 d_F^2)} h_m x_F + u_{mf,P} \frac{(1 - \varepsilon_{mf,P})}{(\varepsilon_{mf,P}^3 d_P^2)} h_0 (1 - x_F)}{\frac{(1 - \varepsilon_{mf,m})}{(\varepsilon_{mf,m}^3 d_{av}^2)} h_m + \frac{(1 - \varepsilon_{mf,P})}{(\varepsilon_{mf,P}^3 d_P^2)} (h_0 - h_m)(1 - x_F)} \quad (10)$$

that relates  $u_{ff}$  of the mixture to the minimum fluidization velocities of its components.

With regard to the Eqs. 8 and 10, the authors have verified that substitution into them of the condition  $x_F = 0$  or  $x_F = 1$  makes  $u_{ff}$  revert to  $u_{mf,P}$  or  $u_{mf,F}$ , a circumstance that indicates how the model keeps its validity even at the extremes of the composition field represented by either mixture component. The relevant demonstration, which resorts to the theorem of de l'Hopital when the right-hand side of either equation becomes undetermined, is here deliberately omitted, to avoid overburdening the article.

As already found with density or size-segregating beds,<sup>1</sup> the height  $h_m$  can be estimated by the following one-parameter correlation

$$\frac{h_m}{h_0} = k \frac{(1 - \varepsilon_{mf,m}) \varepsilon_{mf,P}^3}{(1 - \varepsilon_{mf,P}) \varepsilon_{mf,m}^3} \sqrt{x_F(1 - x_F)}, \quad (11)$$

**Table 1. Properties of the Experimental Solids**

Solid	Density (g/cm <sup>3</sup> )	Sieve Size (μm)	Sauter Mean Diameter (μm)	Experimental <i>u<sub>mf</sub></i> (cm/s)
Molecular sieves (MS)	1.46	710–900	800	31.9
Glass ballotini (GB)	2.48	500–710	624	20.0
		500–600	593	30.8
		250–300	562	24.5
		125–180	271	6.5
		125–180	154	1.8
Ceramics (CE)	3.76	355–400	376	16.7
Steel shots (SS)	7.60	400–450	439	48.6
		200–250	243	14.3
		150–200	170	6.9
Bronze (BR)	8.72	250–300	254	17.5

whose validity is confirmed also for beds of fully dissimilar particulate materials. It is worth reminding that in it,  $k$  is a fitting parameter typical of the specific mixture at hand but independent of its composition, to be determined from the comparison of the predictions of the theoretical Eq. 4 with the experimental curve of  $u_{ff}$  vs.  $x_F$ .

## Experimental

### Equipment

A transparent column with an internal diameter of 10 cm, fed with compressed air, was used in all the fluidization experiments. The gas flow was regulated by a bench of rotameters and admitted to the facility through a plastic porous plate 4-mm thick, capable to ensure even distribution throughout the column section. The total pressure drop across the particle bed was measured by a water manometer connected to a tap located 1 mm above the gas distribution plane, while bed heights were read on three graduated scales spaced at 120° around the column wall and then averaged. These measurements were also used to calculate the voidage of the fixed bed at varying mixture composition as

$$\varepsilon_{0,m} = 1 - \left( \frac{m_F}{\rho_F} + \frac{m_P}{\rho_P} \right) \frac{1}{A h_0} \quad (12)$$

in a way that the dependence of  $\varepsilon_{0,m}$  on the volumetric fraction of either component was determined for each binary system. Following what done in the previous stages of this research,<sup>1,2</sup> data of  $\varepsilon_{0,m}$  were always taken as equal to those of the minimum fluidization voidage  $\varepsilon_{mf,m}$ ; as verified in the past, such an assumption leads to negligible errors, given that none of the beds investigated, made of Geldart's B solids, undergoes expansion when fluidized.

### Solids and mixtures

All the experiments reported in this study used closely sieved cuts of various spherical materials. Determination of

**Table 2. Properties of the Experimental Mixtures**

Type	Mixture (Packed/Fluid)	$\rho_P/\rho_F$ (–)	$d_P/d_F$ (–)	$k$ (–)
Jetsam = packed	CE376-GB271	1.52	1.39	0.65
	MS624-GB154	0.59	4.05	0.14
	SS439-MS800	5.20	0.55	0.37
Flotsam = packed	GB562-BR254	0.28	2.21	0.056
	CE376-SS170	0.49	2.21	0.21
	GB593-SS243	0.33	2.44	0.14

the granulometric distribution of each sample, carried out by a Malvern Mastersizer 2000 laser diffractometer, allowed to calculate its Sauter mean diameter. Solid densities were measured by a Quantachrome helium pycnometer. Both properties are reported in Table 1, together with the minimum fluidization velocity of each solid cut.

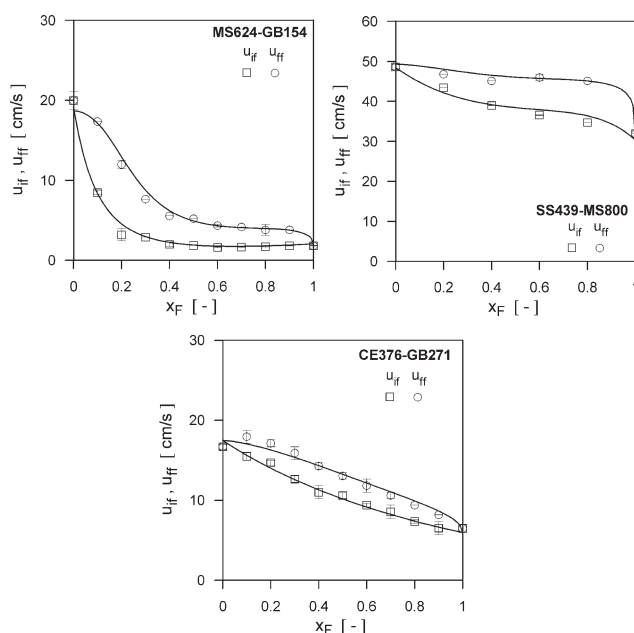
Six binary mixtures were prepared, so as to verify the ability of the model equations to represent the fluidization behavior of two-solid systems in a wide variety of cases. The properties of these mixtures are reported in Table 2: their density ratio ranges from 0.28 to 5.20 while their size ratio varies from 0.55 to 4.10. These intervals are thought to represent the field of practical interest for applications. For three of these mixtures (CE376-GB271, MS624-GB154, and SS439-MS800), the packed component is also the jetsam so that the bed results subjected to the mechanism of top fluidization; for the other three (GB562-BR254, CE376-SS170, and GB593-SS243), the packed solid is the flotsam and bottom fluidization occurs.

In all experiments, the aspect ratio  $h_0/D$  of the fixed bed was initially set equal to 1.7, so that mixture composition was varied by adjusting the mass of its components under this constraint.

## Experimental Results and Model Validation

The substantial diversity between the mechanisms of top and bottom fluidization does not preclude the possibility of characterizing the process of segregating suspension of any two-solid mixture by the same criterion, based on the dependence of the velocities  $u_{if}$  and  $u_{ff}$  on overall bed composition. By performing sets of experiments in which  $x_F$  was let vary at intervals of 0.10, the fluidization diagrams of all binary systems investigated have been reconstructed, so as to test the ability of the model equations proposed in this study to correctly interpret the influence of the various constitutive and operative parameters on system behavior.

With reference to the binary systems listed in Table 2, Figure 4 reports the experimental data of  $u_{if}$  and  $u_{ff}$  of the three systems whose fluidization process starts at the free

**Figure 4. Fluidization diagrams of mixtures whose fluidized component is flotsam.**

Top fluidization.



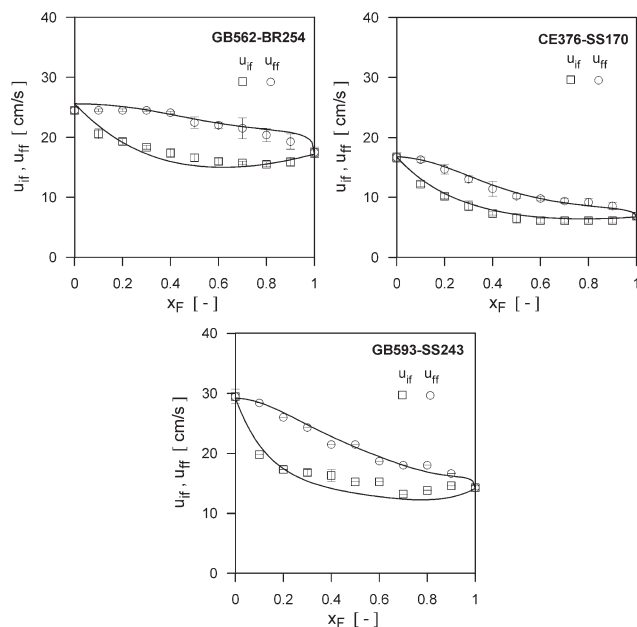


**Figure 5. Fluidization diagrams of mixtures whose fluidized component is jetsam.**

**Bottom fluidization.**

surface of the bed, that is, those whose fluidized component is also the flotsam. The degree of similarity between the shape of each of these diagrams with the typical curves of simple density- or size-segregating beds,<sup>2-5</sup> that always exhibit top fluidization, gives a quick idea of which of the two segregating factors (particle density or size) plays a major role in promoting solid stratification. Thus, a mixture like MS624-GB154, for which the segregating tendency due the high size ratio of the two components ( $d_P/d_F = 4.05$ ) clearly prevails on the counteracting effect of the limited density difference ( $\rho_P/\rho_F = 0.59$ ), has a fluidization diagram very similar to that of size-segregating systems. At the other extreme, for SS439-MS800 the phenomenon of segregation is mostly driven by the density difference between components ( $d_P/d_F = 0.55$ ,  $\rho_P/\rho_F = 5.20$ ), so that the fluidization diagram of the mixture is very close to that of a density-segregating binary bed. When, instead, the effectiveness of the two counteracting segregation factors is comparable, as in the case of the bed CE376-SS170 ( $d_P/d_F = 1.39$ ,  $\rho_P/\rho_F = 1.52$ ), the shape of the experimental diagram of  $u_{if}$  and  $u_{ff}$  results intermediate to those observed in the previous cases.

A similar series of diagrams is presented in Figure 5, that refers to the three systems investigated subjected to the mechanism of bottom fluidization, whose properties are reported in Table 2. Although the properties of the individual solids cover a wide interval of values, the component density ratio  $d_P/d_F$  of these binary beds does not significantly change, whereas the size ratio  $d_P/d_F$  varies from 0.28 to 0.49.

To a different extent all three mixtures undergo the simultaneous but antagonistic effects of density segregation and size segregation, a common feature that explains the similarity of their fluidization diagrams, whose width, measured by the difference  $u_{ff} - u_{if}$  at varying  $x_F$ , is, however, different.

Figures 4 and 5 report also the theoretical trends of the initial and final fluidization velocities as calculated by Eqs. 1 and 10, respectively. Their calculation requires introducing into these equations the experimental data of  $\varepsilon_{mf}$  at varying mixture composition. Such data are reported in Figure 6 for

all binary beds investigated. With the exception of that of the mixture CE376-GB271, whose components do not differ very much in particle diameter, all the curves exhibit a minimum at intermediate compositions, as much pronounced as the size ratio between the two solids increases.

Similar to what illustrated for simple two-density or two-size beds,<sup>1</sup> calculation of  $u_{if}$  by Eqs. 1–3 is thoroughly predictive, as the initial fluidization velocity is determined from the properties of the homogeneous fixed bed and does not involve segregation, which begins to alter component distribution at velocities just higher. The model curves of  $u_{if}$  are reported on each of the diagrams of Figures 4 and 5; for all binary beds under examination, they provide an accurate representation of the lower bound of the fluidization velocity interval.

As regards  $u_{ff}$ , the equally theoretical nature of Eq. 10 is not sufficient to allow an analogous predictive calculation. The difficulty is given by the presence in it of the variable  $h_m$  (the height of the homogeneous portion of the bed at the final fluidization condition) whose determination would require a full understanding of the relationship that links the progress of fluidization to that of segregation of mixture components. As the relationship between the two phenomena is still a problem for fluidization research, solving Eq. 10 requires associating to it a relationship capable to provide the values of  $h_m$  on a different basis. This is done by the semiempirical Eq. 11: in it,  $k$  is a fitting parameter typical of each mixture but independent of its composition, with the value that provides the best fit of the experimental data over the whole field of  $x_F$  after having substituted into the relationship the voidage values of Figure 6.

The theoretical trends of  $u_{ff}$  calculated by Eqs. 10 and 11 are plotted in Figures 4 and 5 and the values of  $k$  relevant to each binary system are reported in Table 2. For all of them, irrespective of the mechanism being that of top or bottom fluidization, the ability of the model to interpret the variation of the final fluidization velocity with mixture composition and voidage variations, as well as its dependence on component properties, is satisfactory. As summarized in Figure 7, where a comparison is made between the experimental measurements of  $u_{ff}$  at all values of  $x_F$  and the corresponding calculated values, the error level is about 10%, fully in line with what encountered in the prediction of the minimum fluidization velocity of monosolid beds.

## Discussion

As they are typical of fluidization of beds of two solids, density and size segregation have been the object of a large

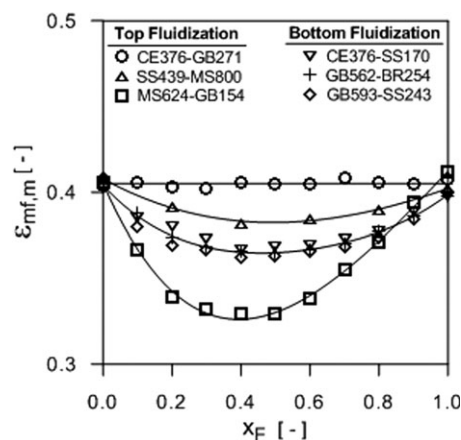


**Figure 6. Voidage of the homogeneous binary beds at varying composition.**

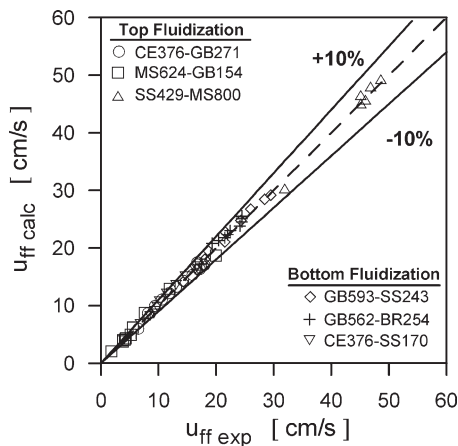


**Figure 7. Comparison between calculated and experimental values of the final fluidization velocity.**

number of studies, mostly devoted to either of the two phenomena. Among them, rather few are those whose authors have proposed quantitative relationships of some effectiveness to link the progress of fluidization to that of component separation.<sup>7–10</sup> The nature of these relationships is, however, essentially empirical, so that even when they prove capable to fit a certain number of data relevant to the fluidization behavior of some specific type of mixture, their applicability to other two-solid systems appears very limited. An immediate consequence of that has been, so far, the difficulty of representing the phenomenology of fluidization of density- and size-segregating mixtures by correlations of the same kind.

Given that, mixtures of thoroughly different solids, which are subjected to both segregation factors, have ended up with constituting a sort of third object of investigation rather than being addressed as systems whose fluidization pattern must combine those of the two elementary systems.

On overcoming these difficulties, the analysis of the forces that act on the layers created by the process of binary fluidization, embodied by Eqs. 1, 10, and 11, brings to a representation whose distinctive feature is that of being applicable to any type of two-solid mixture. It can be verified, to this regard, that while Eq. 11 remains unchanged for all systems, imposition of the condition  $d_F = d_P$  (for simple two-density beds) or  $\rho_F = \rho_P$  (for the case of two-size beds) in Eq. 1 leads, respectively, to the following expressions of the initial fluidization velocity

$$180 \frac{\mu_g u_{if} (1 - \varepsilon_{mf,m})^2}{d^2 \varepsilon_{mf,m}^3} = [(\rho_F - \rho_g)x_F + (\rho_P - \rho_g)(1 - x_P)]g(1 - \varepsilon_{mf,m}) \quad (13)$$

$$180 \frac{\mu_g u_{if} (1 - \varepsilon_{mf,m})^2}{d_{av}^2 \varepsilon_{mf,m}^3} = (\rho - \rho_g)(1 - \varepsilon_{mf,m})g \quad (14)$$

Similarly, whenever the mixture is composed by particles of the same size ( $d_F = d_P$ ) Eq. 10 simplifies to:

$$u_{ff} = \frac{[(\rho_F - \rho_g)x_F h_m + (\rho_P - \rho_g)(1 - x_F)h_0]g \varepsilon_{mf}^3 d^2}{180 \mu_g (1 - \varepsilon_{mf})[h_m + (h_0 - h_m)(1 - x_F)]} \quad (15)$$

whereas with systems made of two cuts of the same material ( $\rho_F = \rho_P$ ) it reduces to

$$u_{ff} = \frac{[x_F h_m + (1 - x_F)h_0](\rho - \rho_g)g}{180 \mu_g \left[ \frac{(1 - \varepsilon_{mf,m})}{(\varepsilon_{mf,m}^3 d_{av}^2)} h_m + \frac{(1 - \varepsilon_{mf,P})}{(\varepsilon_{mf,P}^3 d_P^2)} (h_0 - h_m)(1 - x_F) \right]} \quad (16)$$

successfully validated in a previous stage of the present research.<sup>1</sup>

It can, therefore, be remarked that the equations presented in this article constitute the generalized form of a model that, irrespective of whether the mechanism of suspension starts at the top or at the bottom of the bed, provides a unique theoretical frame for the process of fluidization of any two-solid mixture.

In view of further developments, the model concentrates in the parameter  $k$  the aspects of the problem still unclear, namely the relationship that links the progress of fluidization to that of component segregation; the extent of the latter phenomenon is measured by the value of the residual height  $h_m$  of the original well-mixed particle assembly when the whole bed is fully sustained by the upflowing gas. Although it is not possible, for the time being, to give a really theoretical foundation to Eq. 11 or to define the dependence of  $k$  on the whole set of process variables, the results achieved seem to confirm the possibility of extending the basic concepts of the fluidization theory of monocomponent beds to more complex systems.

Elimination of the recourse to empirical information to model the process of binary fluidization constitutes one of the objectives of future work. That will seemingly require a better understanding of the mixing-segregation equilibrium between mixture components that establishes itself at velocities between  $u_{if}$  and  $u_{ff}$ . Another goal is that of verifying and possibly extending the validity of the results obtained so far with mixtures of spherical solids to beds of practical interest for applications (such as, for instance, combustion and gasification of fossil fuels, biomass, or wastes). This means, in particular, accounting for the influence of the shape of the two components on voidage variations, an issue that has already been shown to play a key role on the overall fluidization behavior of multisolid systems.

## Conclusions

The process of segregating fluidization of a homogeneous mixture of two solids differing in density and size begins at the top of the bed whenever the lighter component is also the smaller whereas, in the opposite case, its start may occur at the bottom of the bed if the denser solid is so small to be the first to be suspended. In the velocity interval bounded by the initial and the final fluidization velocity of the mixture, either mechanism is associated to the continuous change of the axial distribution of the two components, whose pattern is determined by the combined action of the two segregation factors.

Whatever the mechanism of fluidization, the two limiting velocities of the process,  $u_{if}$  and  $u_{ff}$ , are calculated in purely theoretical terms by a force balance referred to the homogeneous and to the partially segregated binary bed, respectively. The latter state is represented by a three-layer structure, an assumption that apparently constitutes a satisfactory approximation of the actual distribution of the two components along the bed axis. Although the calculation of  $u_{if}$  is fully predictive, that of  $u_{ff}$  requires associating to the force balance a simple one-parameter equation, whose function is that of determining the height of the residual portion of the homogeneous mixture at the endpoint of the fluidization process.

The theoretical equations interpret with good accuracy the fluidization behavior of a wide variety of systems of fully dissimilar solids, irrespective of their mechanism of suspension being that of “top” or “bottom fluidization.” Moreover, when applied to the elementary cases of mixtures of solids that differ only in density or size, they revert to the forms already validated in a previous stage of the present research.

On extending the theory of fluidization to two-solid systems, the model provides for the first time a unified representation of the suspension process of all types of mixtures and overcomes, by this way, many of the limitations intrinsic to the empirical approaches adopted so far.

## Notation

$A$  = column cross section,  $\text{cm}^2$   
 $D$  = bed diameter,  $\text{cm}$   
 $d$  = particle diameter,  $\mu\text{m}$   
 $d_{\text{av}}$  = Sauter mean diameter (Eq. 2),  $\mu\text{m}$   
 $F_D$  = drag force,  $\text{g cm/s}^2$   
 $g$  = gravity acceleration,  $\text{cm/s}^2$   
 $h$  = height of the particle layer,  $\text{cm}$   
 $h_0$  = height of the fixed bed,  $\text{cm}$   
 $k$  = best-fit parameter (Eq. 11), -  
 $m$  = mass,  $\text{g}$   
 $u_{\text{if}}, u_{\text{ff}}$  = initial, final fluidization velocity,  $\text{cm/s}$   
 $u_{\text{mf}}$  = minimum fluidization velocity,  $\text{cm/s}$   
 $x$  = volume fraction, -  
 $W$  = buoyant weight of the bed,  $\text{g cm/s}^2$   
 $\varepsilon$  = voidage, -  
 $\varepsilon_0$  = voidage of the fixed bed, -  
 $\varepsilon_{\text{mf}}$  = minimum fluidization voidage, -  
 $\mu_g$  = gas viscosity,  $\text{g/cm s}$   
 $\phi$  = particle sphericity, -  
 $\rho$  = solid density,  $\text{g/cm}^3$   
 $\rho_{\text{av}}$  = average density of the mixture,  $\text{g/cm}^3$   
 $\rho_g$  = gas density,  $\text{g/cm}^3$

## Subscripts

F,P = of the fluidized, packed component (or layer)  
 m = of the homogeneous mixture

## Literature Cited

- Formisani B, Girimonte R, Vivacqua, V. Fluidization of mixtures of two solids differing in density or size. *AIChE J.* 2011;57:2325–2333.
- Formisani B, Girimonte R, Longo, T. The fluidization process of binary mixtures of solids: development of the approach based on the fluidization velocity interval. *Powder Technol.* 2008;185:97–108.
- Chen JL-P, Keairns DL. Particle segregation in a fluidized bed. *Can J Chem Eng.* 1975;53:395–402.
- Vaid RP, Sen Gupta P. Minimum fluidization velocities in beds of mixed solids. *Can J Chem Eng.* 1978;56:292–296.
- Carski M, Pata J, Vesely V, Hartman M. Binary system fluidized bed equilibrium. *Powder Technol.* 1987;51:237–242.
- Rowe PN, Nienow, AW, Agbim A. The mechanism by which particles segregate in gas fluidised beds-binary systems of near-spherical particles. *Trans Inst Chem Eng.* 1972;50:310–323.
- Nienow AW, Rowe PN, Cheung LY-L. A quantitative analysis of the mixing of two segregated powders of different density in a gas fluidized bed. *Powder Technol.* 1978;20:89–97.
- Rice RW, Brainovich JF. Mixing/segregation in two- and three-dimensional fluidized beds: binary systems of equidensity spherical particles. *AIChE J.* 1986;32:7–16.
- Wu SY, Baeyens J. Segregation by size difference in gas fluidized beds. *Powder Technol.* 1998;98:139–150.
- Peeler JPK, Huang JR. Segregation of wide size range particle mixtures in fluidized beds. *Chem Eng Sci.* 1989;44:1113–1119.

Manuscript received Nov. 2, 2011, and revision received May 9, 2012.